

# Lawrence Berkeley National Laboratory

## Lawrence Berkeley National Laboratory

### **Title**

THE KINETICS AND MECHANISM OF CARBON MONOXIDE HYDROGENATION OVER ALUMINA-SUPPORTED RUTHENIUM

### **Permalink**

<https://escholarship.org/uc/item/5fj0w7vj>

### **Author**

Kellner, C. Stephen

### **Publication Date**

1980-12-01



# Lawrence Berkeley Laboratory

UNIVERSITY OF CALIFORNIA

## Materials & Molecular Research Division

Submitted to the Journal of Catalysis

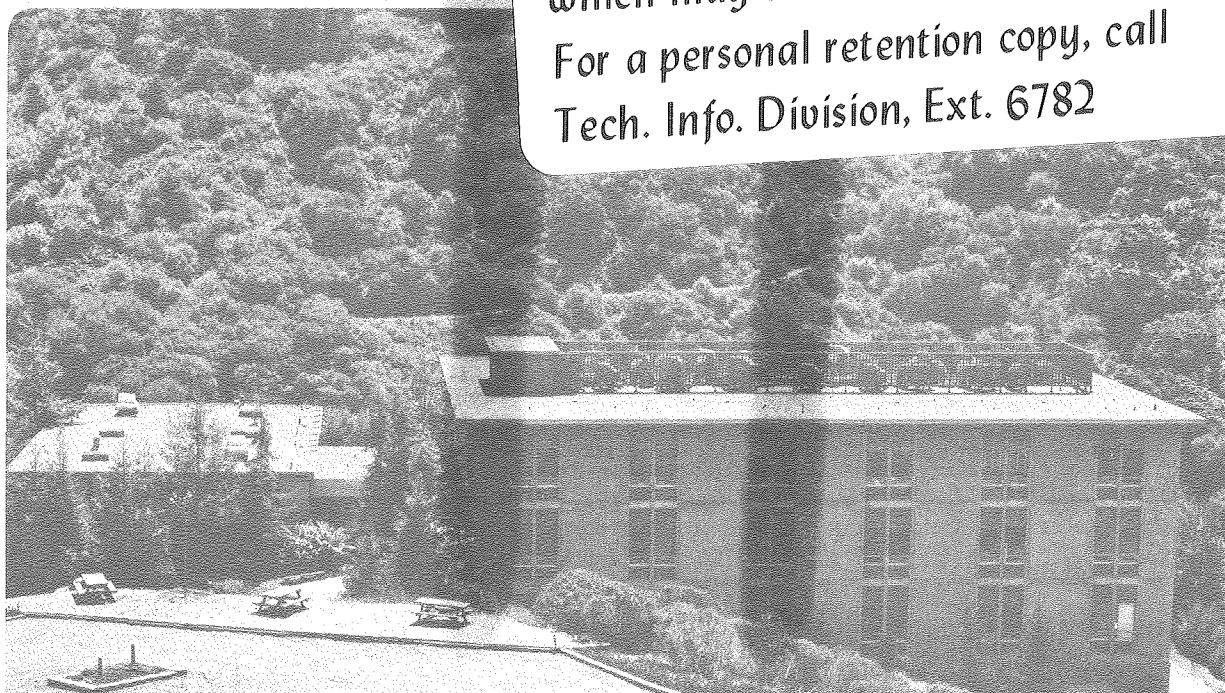
THE KINETICS AND MECHANISM OF CARBON MONOXIDE  
HYDROGENATION OVER ALUMINA-SUPPORTED RUTHENIUM

C. Stephen Kellner and Alexis T. Bell

December 1980

**TWO-WEEK LOAN COPY**

This is a Library Circulating Copy  
which may be borrowed for two weeks.  
For a personal retention copy, call  
Tech. Info. Division, Ext. 6782



LBL-12133  
c.2

## DISCLAIMER

This document was prepared as an account of work sponsored by the United States Government. While this document is believed to contain correct information, neither the United States Government nor any agency thereof, nor the Regents of the University of California, nor any of their employees, makes any warranty, express or implied, or assumes any legal responsibility for the accuracy, completeness, or usefulness of any information, apparatus, product, or process disclosed, or represents that its use would not infringe privately owned rights. Reference herein to any specific commercial product, process, or service by its trade name, trademark, manufacturer, or otherwise, does not necessarily constitute or imply its endorsement, recommendation, or favoring by the United States Government or any agency thereof, or the Regents of the University of California. The views and opinions of authors expressed herein do not necessarily state or reflect those of the United States Government or any agency thereof or the Regents of the University of California.

The Kinetics and Mechanism of Carbon Monoxide  
Hydrogenation Over Alumina-Supported Ruthenium

by

C. Stephen Kellner and Alexis T. Bell

Materials and Molecular Research Division  
Lawrence Berkeley Laboratory

and

Department of Chemical Engineering  
University of California, Berkeley, California 94720

Submitted to

Journal of Catalysis

## ABSTRACT

A study was conducted of hydrocarbon synthesis from CO and H<sub>2</sub> over an alumina-supported Ru catalyst. Rate data for the formation of methane and C<sub>2</sub> through C<sub>10</sub> olefins and paraffins were fitted by power law rate expressions. The kinetics observed experimentally can be interpreted in terms of a comprehensive mechanism for CO hydrogenation, in which CH<sub>x</sub> (x=0-3) species play a primary role. Expressions for the kinetics of methane synthesis, the kinetics and distribution of C<sub>2+</sub> olefins and paraffins, and the probability of hydrocarbon chain growth derived from this mechanism are found to be in good agreement with the experimental results. The observed deviations from theory can be ascribed to secondary processes such as olefin hydrogenation and paraffin hydrogenolysis.

## INTRODUCTION

During the past decade, extensive efforts have been made to understand the mechanism by which Group VIII metals catalyze the synthesis of hydrocarbons from CO and H<sub>2</sub> (1-7). One of the most important results of these investigations has been to draw attention to the importance of nonoxygenated surface intermediates. An increasing body of evidence now supports the hypothesis that hydrocarbon synthesis is initiated by the dissociation of CO and that the carbon atoms thus produced are hydrogenated to form adsorbed methylene and methyl groups. It has been proposed (5-7) that methyl groups act as precursors for the formation of methane as well as the growth of hydrocarbon chains, the latter process beginning with the insertion of a methylene group into the metal-carbon bond of a methyl group. Chain growth can continue by the further addition of methylene units to adsorbed alkyl species. Olefins and paraffins are finally produced from the alkyl moieties by either hydrogen elimination or addition.

A substantial part of the evidence supporting this view of hydrocarbon synthesis has been obtained from studies conducted with ruthenium catalysts. The emphasis on this metal can be explained by the fact that ruthenium produces, primarily, linear olefins and paraffins and relatively few oxygenated products. Moreover, unlike iron and cobalt, ruthenium is not converted to a carbide under reaction conditions. Studies by several authors (8-11) have shown that chemisorbed CO will dissociate on ruthenium at elevated temperatures to form adsorbed carbon atoms. Hydrogenation of this carbon occurs very readily to form methane as well as higher molecular weight paraffins. Ekerdt and Bell (12) have shown that carbon deposition also takes place during the steady-state reaction of CO and H<sub>2</sub>, and that hydrogenation of this carbonaceous deposit following the elimination of chemisorbed CO produces a spectrum of hydrocarbon products. These latter

results demonstrate that chain growth can occur in the absence of adsorbed CO. Further evidence for the participation of atomic carbon in the growth of hydrocarbon chains has been obtained by Biloen et al. (11). In these studies nickel, cobalt, and ruthenium catalysts were precovered with  $^{13}\text{C}$  atoms produced by the disproportionation of  $^{13}\text{CO}$ . The adsorbed  $^{13}\text{CO}$  was exchanged with  $^{12}\text{CO}$  and the catalysts were then exposed to a mixture of  $^{12}\text{CO}$  and  $\text{H}_2$ . Careful mass spectrometric analysis of the products showed a random distribution of  $^{12}\text{C}$  and  $^{13}\text{C}$  among the hydrocarbons, consistent with the initial inventories of the two isotopes. It was also found that the time needed to convert  $^{13}\text{C}$  atoms and  $^{12}\text{CO}$  molecules to methane were nearly identical. From these observations it was concluded that CO dissociation is very rapid and hence is unlikely to be a rate limiting step, that  $\text{CH}_x$  ( $x = 0-3$ ) species constitute the most reactive  $\text{C}_1$  surface species, and that methane and other hydrocarbons are formed from the same building blocks. These conclusions have also been supported by the analysis of methane synthesis kinetics reported by Ekerdt and Bell (12) and by the observation of a significant inverse  $\text{H}_2/\text{D}_2$  isotope effect on methane synthesis recently reported by Kellner and Bell (13).

The proposition that hydrocarbon chain growth can occur on a ruthenium surface via a polymerization mechanism involving methylene groups as the monomer has recently been supported by the work of Brady and Petit (14). These authors demonstrated that a spectrum of hydrocarbons, resembling that obtained by CO hydrogenation, can be formed by reaction of  $\text{CH}_2\text{N}_2$  and  $\text{H}_2$  over ruthenium and other Groups VIII metals. The results were explained by suggesting that the decomposition of  $\text{CH}_2\text{N}_2$  acts as a source of methylene groups, a part of which is converted to methyl groups by reaction with adsorbed hydrogen. It was proposed that the methyl groups then act as initiators for chain growth. The applicability of these results and their

interpretation to hydrocarbon synthesis from CO and H<sub>2</sub> is supported by the work of Bell and coworkers (15,16). Their work has shown that methyl, methylene, and higher molecular weight alkyls present on a ruthenium surface can be detected through the reaction of these species with olefins, and that the consumption of surface methylene groups by this means inhibits the propagation of hydrocarbon chain growth.

In the present study an investigation has been carried out of the kinetics of hydrocarbon synthesis over an alumina-supported ruthenium catalyst. Emphasis was placed on establishing the influence of reaction conditions on the rates of product formation, the distribution of olefins and paraffins according to carbon number, and the ratio of olefin to paraffin obtained for each carbon number. These data were then used to evaluate theoretical expressions for the reaction kinetics, derived from a comprehensive mechanism for hydrocarbon synthesis.

#### EXPERIMENTAL

A 1% Ru/Al<sub>2</sub>O<sub>3</sub> catalyst was prepared by adsorption of Ru<sub>6</sub>C(CO)<sub>17</sub> from pentane solution on to Kaiser KA-201  $\gamma$ -alumina. Details concerning synthesis of the complex and the impregnation procedure have been described previously (17). Once dried, the catalyst was reduced in flowing H<sub>2</sub>. Reduction was begun slowly raising the temperature from 298 to 673 K and continued by maintaining it at 673 K for 8 hr. The dispersion of the reduced catalyst was determined to be 1.0 by H<sub>2</sub> chemisorption.

A stainless steel microreactor heated in a fluidized bed was used for all of the work reported here. Reactants were supplied from a high-pressure cylinder containing a desired ratio of H<sub>2</sub> and CO. The reaction products were analyzed by gas chromatography using flame ionization detection. A balanced pair of 2.4 mm by 1 m stainless steel



columns packed with Chromsorb 106 was used to separate  $C_1$  through  $C_5$  paraffins and olefins. A 0.25 mm by 35 m glass capillary column coated with OV-101 was used to separate  $C_5$  through  $C_{10}$  paraffins and olefins. Complete product distributions were determined by normalizing the analyses for the  $C_5$  products obtained from the packed and capillary columns.

Prior to each series of experiments, the catalyst (100 mg) was reduced in flowing  $H_2$  for 10 to 12 hr at 673 K and 10 atm. The temperature was then lowered to 498 K and the feed mixture was introduced at a flow rate of  $200 \text{ cm}^3/\text{min}$  (NTP). Ten minutes after the reaction had begun, a gas sample was taken for analysis and the gas feed was switched over to pure  $H_2$  for 1 hr. By alternating short reaction periods and longer reduction periods, a stable catalyst activity could be achieved after several cycles. Once this condition had been obtained the reaction conditions were adjusted to those desired for a particular experiment. Periodically, data were taken at 498 K, 10 atm, and  $H_2/CO = 3$  to determine whether changes in catalyst activity had occurred. In all cases, activities were reproduced to within a few percent. Maintaining the catalyst in  $H_2$  for prolonged periods was also determined to have no effect on catalyst activity.

## RESULTS

The rate of methane formation was measured at pressures between 1 and 10 atm, temperatures between 448 and 548, and  $H_2/CO$  ratios of 1, 2, and 3. The accumulated data were fitted, by means of a nonlinear least squares regression, to the power law expression given by eqn. 1,

$$N_{C_1} = 1.3 \times 10^9 \exp(-28,000/RT) P_{H_2}^{1.35} / P_{CO}^{0.99} \quad (1)$$

In this equation,  $N_{C_1}$  is the rate of methane formation per second per surface Ru site, and  $P_{H_2}$  and  $P_{CO}$  are the partial pressures of  $H_2$  and  $CO$ ,

respectively, expressed in atmospheres. Figure 1 illustrates the quality of agreement between rates calculated using eqn. 1 and those determined experimentally. The average deviation between experiment and correlation is less than  $\pm 6\%$ .

Seventy to eighty percent of the hydrocarbon products were analyzed to be  $C_2$  through  $C_{10}$  paraffins and olefins. Examples of the ratio of the formation of hydrocarbons containing  $n$  carbon atoms to the rate of methane formation are shown in Figs. 2 and 3. Figure 2 shows that with the exception of the points for  $n=2$  all of the data taken at 1 atm lie along straight lines on the coordinates of  $\log (N_{C_n} / N_{C_1})$  versus  $(n-1)$ . The decreasing slope of the lines as either the  $H_2/CO$  ratio or the temperature is decreased is indicative of an increase in the average molecular weight of the products. The data taken at 10 atm (Fig. 3) also lie along straight lines on the indicated coordinates, but in this case deviations are seen for  $n = 2$  and 3. When either the  $H_2/CO$  ratio or the temperature is decreased, the slope of the lines in Fig. 3 decrease slightly, and the lines appear to be translated upwards in a near parallel fashion.

The kinetics for the synthesis of  $C_2$  through  $C_{10}$  olefins and paraffins can also be represented by power law rate expressions. Parameter values obtained by fitting the data to such expression are presented in Tables I and II. Examination of Table I shows that a positive order dependence on  $H_2$  and a negative order dependence on CO partial pressures is observed in all cases. For a given carbon number, the  $H_2$  dependence for paraffin formation is higher than that for olefin formation, whereas the CO dependence is more nearly the same for both products. The data in Table II also indicate that the magnitudes of  $m$  and  $n$  for the formation of olefins decrease substantially with increasing carbon number. While there is some indication of a similar trend for the paraffins, the pattern is not as clearly evident as for the olefins.

The information presented in Table II shows that the activation energy for olefin synthesis is higher than that for paraffin synthesis, suggesting that the olefin to paraffin ratio in the products should increase with increasing temperature. The extent to which this trend is observed is illustrated in Fig. 4. Below about 498K, the plots of  $\log(N_{C_n}^{\bar{=}}/N_{C_n}^{\bar{-}})$  versus  $1/T$  are linear for  $n = 2, 3$ , and 4. From the slope of this portion of the plots, the difference in activation energies for the formation of olefins and paraffins is estimated to be about 6 kcal/mole. The sharp decline in  $\log(N_{C_n}^{\bar{=}}/N_{C_n}^{\bar{-}})$  which occurs at temperatures above 498K can be ascribed to hydrogenation of the olefins. This interpretation was confirmed by examining the effects of reactant space velocity on the olefin to paraffin ratio. At temperatures below 498K, this ratio is independent of space velocity, but as the temperature is increased above 498K, the ratio of olefins to paraffins decreases with decreasing space velocity.

Since it has been reported that olefins formed via primary reactions can be reincorporated to form higher molecular weight products (7,15), an investigation was made to establish the possible influence of such reactions on the observed product distributions. When ethylene was added to the synthesis gas at levels similar to those produced by the reaction, no evidence could be observed for olefin reincorporation. Raising the level of ethylene addition to 0.5 or 1.0% of the total feed (20 to 40 times that normally found in the reaction products) did produce an effect on the distribution of products, as can be seen in Fig. 5. The formation of  $C_3$  and  $C_4$  products is increased, but the formation of  $C_{6+}$  products is suppressed. The extent to which these changes occur increases with the level of ethylene addition. A similar trend was also observed for data taken at 1 atm and 498K.

## DISCUSSION

The kinetics of hydrocarbon synthesis presented here can be interpreted in terms of the mechanism shown in Fig. 6. Detailed discussions of the experimental evidence supporting this view of CO hydrogenation have recently been presented in a number of reviews (1-7). Consequently, the justification for including particular steps, and for assuming that certain of these are reversible, will be restricted to ruthenium.

It is proposed that CO is first adsorbed into a molecular state from which dissociative adsorption can then occur. Infrared studies reported by a number of authors (12,18-20) indicate that the surface of Ru is nearly saturated by molecularly adsorbed CO under reaction conditions. The reversibility of molecular adsorption is supported by recent isotopic substitution studies performed with  $^{12}\text{CO}$  and  $^{13}\text{CO}$  which indicate that equilibration of the surface with the gas phase is very rapid under reaction conditions (21). Low and Bell (10) have shown that CO disproportionation will occur to a significant degree over  $\text{Ru}/\text{Al}_2\text{O}_3$  for temperatures in excess of 423K. These results suggest that CO dissociation is an activated process. More recently, TPD experiments performed by McCarty and Wise (22) have demonstrated that the recombination of carbon and oxygen atoms and the desorption of CO are very rapid since extensive scrambling of preadsorbed  $^{13}\text{C}^{16}\text{O}$  and  $^{12}\text{C}^{18}\text{O}$  was observed at temperatures above 473K, where hydrocarbon synthesis normally occurs.

The adsorption of  $\text{H}_2$  is assumed to occur dissociatively, and to be reversible. This view is supported by  $\text{H}_2/\text{D}_2$  scrambling studies performed in the presence of CO over a  $\text{Ru}/\text{SiO}_2$  catalyst (21). The results of these experiments show that above 423K, the extent of scrambling is very close to that predicted at equilibrium, indicating that the rates of  $\text{H}_2(\text{D}_2)$  adsorption, reaction, and desorption are faster than the rate of hydrocarbon synthesis.

It is well recognized that during CO hydrogenation over Ru, water is the primary product via which oxygen is removed from the catalyst surface (12). The mechanism of forming water in the presence of substantial amounts of adsorbed CO is not known and may occur via either a sequence of Langmuir-Hinshelwood steps or a concerted Rideal-Eley step. For the purposes of the present discussion it has been assumed that the latter process represents the dominant reaction path.

The stepwise hydrogenation of single carbon atoms is taken as the starting point for hydrocarbon synthesis. Studies by a number of investigators (9-11) have shown that atomic carbon produced by either CO disproportionation or CO hydrogenation is extremely reactive and will form methane and higher molecular weight hydrocarbons upon hydrogenation. Furthermore, the work of Biloen et al. (11) has demonstrated that the incorporation of carbon into hydrocarbons occurs with equivalent ease from molecularly adsorbed CO and atomically adsorbed C, indicating that the dissociation of adsorbed CO is not a rate limiting step in the formation of hydrocarbons. This conclusion is supported further by the recent studies of Kellner and Bell (13) in which evidence was reported for a strong inverse  $H_2/D_2$  isotope effect on the synthesis of methane over two Ru/ $Al_2O_3$  catalysts and a similar albeit weaker effect for synthesis over a Ru/ $SiO_2$  catalyst. The authors noted that the more rapid formation of  $CD_4$  than  $CH_4$  indicates that one or more of the elementary steps preceding the rate limiting step involves the addition of hydrogen and is at equilibrium (e.g., steps 5 through 7).

The methyl groups produced in step 7 are precursors to the formation of methane and the growth of hydrocarbon chains. The former process occurs by the addition of a hydrogen atom to the methyl group and the latter by the insertion of a methylene group into the metal-carbon

bond of the methyl group. Once started, chain growth can continue by further addition of methylene units to the alkyl intermediates. Termination of chain growth is postulated to occur via one of two processes - hydrogen addition to form normal alkanes and  $\beta$ -elimination of hydrogen to form  $\alpha$ -olefins. Thus, one may visualize the formation of  $C_{2+}$  hydrocarbons as a polymerization process in which methylene groups act as the monomer and the alkyl groups are the active centers for chain growth.

The proposed mechanism of methanation and chain growth is strongly supported by the results of several recent studies. Brady and Petit (14) have demonstrated that hydrocarbons can be formed by the decomposition of diazomethane over supported Ru, as well as other Group VIII metals. In the absence of  $H_2$ , ethylene is the only product observed. When  $H_2$  is added to the flow of  $CH_2N_2$ , a product distribution resembling that observed during CO hydrogenation is obtained. The authors propose that methylene groups produced by the decomposition of  $CH_2N_2$  react in the absence of adsorbed hydrogen to form ethylene. In the presence of adsorbed hydrogen, methyl groups are formed. The addition of methylene units to these species initiates chain growth. Direct evidence for the presence of methylene and  $C_1$  through  $C_4$  alkyl groups on the surface of Ru have recently been obtained using the technique of reactive scavenging (15,16). In these studies a small amount of cyclohexene is added to the synthesis gas. The products are observed to contain norcarane; methylcyclohexene; and methyl-, ethyl-, propyl-, and butylcyclohexane in addition to the usual spectrum of hydrocarbons obtained by CO hydrogenation. The appearance of products derived from cyclohexene is explained by the reaction of cyclohexene with methylene and alkyl groups, formed on the catalyst surface from CO and  $H_2$ .

Rate expressions describing the kinetics of forming methane and higher molecular weight hydrocarbons can be derived on the basis of the mechanism shown in Fig. 6, following the introduction of a number of simplifying assumptions. To begin with, it is assumed that the rate of methane formation is controlled by step 8 and that the steps preceding it are at equilibrium. This assumption is supported by the observation of a significant inverse  $H_2/D_2$  isotope effect on the rate of methane formation over a  $Ru/Al_2O_3$  catalyst identical to that used in the present studies (13). Next, it is assumed that steps 9, 10, and 11 are irreversible and that the rate coefficients for these steps are independent of the chain length,  $n$ . The validity of this assumption will be discussed following the derivation of rate expressions for  $C_{2+}$  hydrocarbons. Finally, it will be assumed that the fraction of vacant surface sites can be expressed as

$$\theta_v = \frac{1}{K_1 P_{CO}}, \quad (1)$$

where  $K_1$  is the equilibrium constant for reaction 1. Equation 1 is based on the infrared observations reported by Kellner and Bell (20) which show that under reaction conditions the Ru surface sites active in hydrocarbon synthesis are virtually saturated by linearly adsorbed CO and that the surface coverage by this species can be represented by a Langmuir isotherm which only involves the partial pressure of CO.

The turnover number for methane formation,  $N_{C_1}$ , can be written as

$$N_{C_1} = k_8 \theta_{CH_3} \theta_H, \quad (2)$$

where  $k_8$  is the rate coefficient for step 8 in Fig. 6,  $\theta_{CH_3}$  is the fractional coverage of the Ru surface by  $CH_3$  groups, and  $\theta_H$  is the fractional coverage by H atoms. Since equilibrium has been assumed for steps 1 through 3 and 5 through 7,  $\theta_{CH_3}$  can be expressed as

$$\theta_{\text{CH}_3} = K_2 K_3^{1.5} K_5 K_6 K_7 P_{\text{H}_2}^{1.5} \theta_v / \theta_0 \quad (3)$$

where  $K_i$  is the equilibrium constant for the  $i$ -th reaction and  $\theta_0$  is the fractional coverage of the Ru surface by O atoms. The magnitude of  $\theta_H$  is given by

$$\theta_H = K_3^{1/2} P_{\text{H}_2}^{1/2} \theta_v \quad (4)$$

Substitution of eqn. 3 and 4 into eqn. 2 and introduction of eqn. 1 for  $\theta_v$  results in

$$N_{\text{C}_1} = k_8 \frac{K_2 K_3^2 K_5 K_6 K_7}{K_1^2 \theta_0} \frac{P_{\text{H}_2}^2}{P_{\text{CO}}^2} \quad (5)$$

The dependence of  $N_{\text{C}_1}$  on  $\theta_0$  can be eliminated from eqn. 5 if it is assumed that all of the carbon and oxygen released in step 2, which does not recombine to form adsorbed CO, reacts to form hydrocarbons and water. This implies that

$$N_{\text{H}_2\text{O}} = \sum_{n=1}^{\infty} n N_{\text{C}_n} \quad (6)$$

where

$$N_{\text{H}_2\text{O}} = k_4 \theta_0 P_{\text{H}_2} \quad (7)$$

Since all hydrocarbon products containing two or more carbon atoms must be formed by chain growth, step 9, the overall rate of carbon consumption for the formation of hydrocarbon products can be expressed as

$$\sum_{n=1}^{\infty} n N_{\text{C}_n} = k_8 \theta_{\text{CH}_3} \theta_H + \sum_{n=1}^{\infty} k_p \theta_{\text{CH}_2} \theta_n \quad (8)$$

where  $k_p$  is the rate constant for chain growth, step 9;  $\theta_{\text{CH}_2}$  is the fractional coverage of the Ru surface by methylene groups; and  $\theta_n$  is the fractional coverage of the Ru surface by alkyl groups of chain length  $n$ . Combining eqns. 6, 7, and 8 results in eqn. 9.



$$k_4 \theta_0 P_{H_2} = k_8 \theta_{CH_3} \theta_H + \sum_{n=1}^{\infty} k_p \theta_{CH_2} \theta_n \quad (9)$$

Equation 9 can be solved for  $\theta_0$  in the limits where either methane or higher molecular weight products predominate. For the first case

$N_{C_1} \gg \sum_{n=2}^{\infty} n N_{C_n}$ . Substitution of the expressions for  $\theta_{CH_3}$  and  $\theta_H$  into eqn. 9 results in

$$\theta_0 = \frac{K_3}{K_1} \left( \frac{k_8}{k_4} K_2 K_5 K_6 K_7 \right)^{1/2} \frac{P_{H_2}^{1/2}}{P_{CO}} \quad (10)$$

which, on substitution into eqn. 5, gives

$$N_{C_1} = k_e \frac{P_{H_2}^{1.5}}{P_{CO}} \quad (11)$$

where

$$k_e = \frac{K_3}{K_1} (k_8 k_4 K_2 K_5 K_6 K_7)^{1/2} \quad (12)$$

This result is identical to that obtained by Ekerdt and Bell (12).

For the second case, it is assumed that  $N_{C_1} \ll \sum_{n=2}^{\infty} n N_{C_n}$  so that the first term on the right-hand-side of eqn. 9 can be neglected. To solve for  $\theta_0$  in this case requires the development of expressions for  $\theta_{CH_2}$  and  $\theta_n$ . An expression for  $\theta_{CH_2}$  can be derived from the equilibrium relationships existing between steps 1, 2, 3, 5 and 6. Thus

$$\theta_{CH_2} = \frac{K_2 K_3 K_5 K_6}{K_1 \theta_0} \frac{P_{H_2}}{P_{CO}} \quad (13)$$

An expression for  $\theta_n$  can be obtained by imposing a steady-state balance on the formation of alkyl groups containing n carbon atoms.

$$0 = k_p \theta_{n-1} \theta_{CH_2} - k_p \theta_n \theta_{CH_2} - k_{tp} \theta_n \theta_H - k_{to} \theta_n \theta_v \quad (14)$$

where  $k_{to}$  and  $k_{tp}$  are the rate coefficients for the formation of olefins and paraffins, steps 10 and 11 in Fig. 6. Solving for  $\theta_n$  results in

$$\theta_n = \frac{k_p^\theta \text{CH}_2^\theta \theta_{n-1}}{k_p^\theta \text{CH}_2^\theta + k_{tp}^\theta \text{H} + k_{to}^\theta \text{v}} \quad (15)$$

Equation 15 can be rewritten in terms of the probability of chain propagation,  $\alpha$ , as

$$\theta_n = \alpha^{n-1} \theta_{\text{CH}_3} \quad (16)$$

Comparing eqns. 15 and 16 shows that

$$\alpha = \frac{k_p^\theta \text{CH}_2^\theta}{k_p^\theta \text{CH}_2^\theta + k_{to}^\theta \text{v} + k_{tp}^\theta \text{H}} \quad (17)$$

The sum  $\sum_{n=1}^{\infty} \theta_n$ , appearing in eqn. 9, can now be expressed in closed form as

$$\sum_{n=1}^{\infty} \theta_n = \frac{\theta_1}{(1-\alpha)} \quad (18)$$

If  $\alpha$  is taken to be independent of  $P_{\text{H}_2}$  and  $P_{\text{CO}}$ , an assumption which is not rigorously correct but does not lead to significant error, then an expression for  $\theta_0$  can be obtained by substitution of eqns. 13 and 18 into eqn. 9. Thus,

$$\theta_0 = \left[ \frac{k_p^2 K_2^{2.5} K_3^2 K_5^2 K_6^2 K_7^2}{k_4 K_1^2 (1-\alpha)} \right]^{0.33} \frac{P_{\text{H}_2}^{0.5}}{P_{\text{CO}}^{0.67}} \quad (19)$$

Finally, substitution of eqn. 19 into eqn. 5 results in

$$N_{\text{C}_1} = k_e P_{\text{H}_2}^{1.5} / P_{\text{CO}}^{1.33} \quad (20)$$

where

$$k_e = k_8 \left[ \frac{k_4 K_2^{2.5} K_3^2 K_5^2 K_6^2 K_7^2 (1-\alpha)}{k_p^4 K_1^4} \right]^{0.33} \quad (21)$$

Table III presents a comparison between the predicted dependencies of  $N_{C_1}$  on the partial pressures of  $H_2$  and CO and the dependencies determined from experimental data. It is apparent that the  $H_2$  dependence contained in both limiting forms of the expression derived for  $N_{C_1}$  is in excellent agreement with that observed in this study, as well as others. The first of the two limiting forms for  $N_{C_1}$  also provides an accurate description of the CO dependence determined from the data taken in this study. It should be noted however that while Dalla Betta and Shelef (23) have also noted an inverse first order CO dependence, other investigators (12,24) have found that the inverse dependence is less than first order.

Table III also presents a comparison between the apparent activation energies and preexponential factors for methane formation determined from the present results and those reported by previous investigators. It is seen that the activation energy determined in this study is about 4 kcal/mole higher than that reported earlier. At present there is no explanation for this difference. A substantial variation is observed in the values of the preexponential factors reported by different authors. It is conceivable that a major part of these differences may be related to the precision used in measuring the Ru dispersion and to the effects of dispersion on catalyst activity. As noted by King (25), and Kellner and Bell (26), the specific activity of Ru decreases as the dispersion of the metal increases.

Expressions describing the rates of formation of higher molecular weight products can be derived in a manner similar to that followed in developing an expression for the rate of methane formation. The turnover frequencies for the formation of normal paraffins and  $\alpha$ -olefins can be expressed as follows:

$$N_{C_n}^- = k_{tp} \theta_H \theta_n \quad (22)$$

$$N_{C_n}^= = k_{to} \theta_v \theta_n \quad (23)$$

Summing eqns. 22 and 23 to obtain an expression for the rate of formation of products containing n carbon atoms and substituting from eqn. 16 for  $\theta_n$  results in

$$N_{C_n} = (k_{to} \theta_v + k_{tp} \theta_H) \alpha^{n-1} \theta_{CH_3} \quad (24)$$

Substitution of  $\theta_{CH_3}$  by  $N_{C_1} / (k_8 \theta_H)$  and substitution from eqns. 1 and 4 for  $\theta_v$  and  $\theta_H$  leads to

$$N_{C_n} = (1 + \beta/P_{H_2}^{0.5}) \alpha^{n-1} N_{C_1}, \quad (25)$$

assuming that  $k_{tp} = k_8$ . The parameter  $\beta$  appearing in eqn. 25 is defined as

$$\beta = \frac{k_{to}}{k_{tp} K_3^{1/2}} \quad (26)$$

and is related to the ratio of olefin to paraffin formation in the following fashion:

$$\frac{N_{C_n}^=}{N_{C_n}^-} = \beta/P_{H_2}^{0.5} \quad (27)$$

The form of eqn. 25 suggests that a plot of  $\log(N_{C_n} / N_{C_1})$  versus  $(n-1)$  should be a straight line with a slope given by  $\log \alpha$ . The results presented in Figs. 2 and 3 were plotted in this fashion. As was noted earlier, with the exception of the point for  $n = 2$ , the data taken at 1 atm are in good agreement with eqn. 25. At 10 atm, eqn. 25 also provides a good description of the data, with the exception of the points at  $n = 2$  and 3.

A more complete discussion of the slope of the lines shown in Figs. 2 and 3, and its dependence on reaction conditions, will be presented below.

It is of interest at this point to consider whether the kinetics represented by eqn. 25 are consistent with the type of product distribution described by Friedel and Anderson (27) and Henrici-Olivé and Olive (28). According to these authors the fraction of the total carbon converted to hydrocarbons which contain  $n$  carbon atoms,  $f_n$ , should be given by

$$f_n = n\alpha^{n-1}(1-\alpha)^2 \quad (28)$$

and, consequently, a plot of  $\log(f_n/n)$  versus  $n$  should be a straight line of slope  $\alpha$  and intercept  $\log[(1-\alpha)^2/\alpha]$ . The derivation of eqn. 28, which is often referred to as a Schultz-Flory distribution in the recent literature on Fischer-Tropsch synthesis (28-34), is based on the assumption that chain growth occurs by the addition of single carbon intermediates and that chain termination leads to the formation of stable products. No regard need be given in this derivation to the details of the chain propagation or termination steps.

The expressions contained in eqn. 25 for the kinetics of olefin and paraffin synthesis are consistent with a Schulz-Flory distribution, provided one considers products of a homologous series, viz. only olefins or paraffins. This statement can be verified by starting out with the defining equations for the fraction of products within a homologous series, which contain a given number of carbon atoms.

$$f_n^- = \frac{nN_{C_n^-}}{\sum_{n=1}^{\infty} nN_{C_n^-}} \quad (29)$$

$$f_n^{\bar{}} = \frac{nN_{C_n}^{\bar{}}}{\sum_{n=2}^{\infty} nN_{C_n}^{\bar{}}} \quad (30)$$

Notice that the summation for paraffins runs from one to infinity while that for olefins runs from two to infinity. Substitution of the first and second terms of eqn. 25 into eqns. 29 and 30, respectively, gives

$$f_n^{\bar{}} = n \alpha^{(n-1)} (1-\alpha)^2 \quad (31)$$

$$f_n^{\bar{}} = \frac{n\alpha^{(n-1)} (1-\alpha)^2}{1 - (1-\alpha)^2} \quad (32)$$

Equation 31 and the numerator of eqn. 32 are identical to eqn. 28. The denominator appearing in eqn. 32 arises from the fact that the summation in eqn. 30 begins with  $n = 2$ .

Figures 7 and 8 illustrate plots of  $f_n^{\bar{}}/n$  and  $f_n^{\bar{}}/n$  versus  $(n-1)$  for data obtained at 1 and 10 atm. Both figures show that, with the exception of the point at  $n = 2$ , the experimental values of  $f_n^{\bar{}}/n$  fall along a straight line. The slope of the line is equal to  $\log \alpha$ , and, as can be seen in Table IV, the values of  $\alpha$  determined from Figs. 7 and 8 are very close to those determined from plots of  $N_{C_n}/N_{C_1}$ . Equation 30 can be tested further by comparing the intercept of the line passed through experimental values of  $f_n^{\bar{}}/n$  with the expression  $(1-\alpha)^2/[1-(1-\alpha)^2]$  obtained from eqn. 30 for  $(n-1) = 0$ . Table IV indicates that the intercepts evaluated from Figs. 7 and 8 are somewhat larger than those predicted by eqn. 30. This difference can be explained if it is assumed that the low value of  $f_2^{\bar{}}/2$  is due to a partial conversion of ethylene to ethane. Under this circumstance the difference between  $2\alpha(1-\alpha)^2/[1-(1-\alpha)^2]$  and the experimentally observed value of  $f_2^{\bar{}}/2$  would correspond to the carbon number fraction of the ethylene converted to ethane. Imposing this correction leads to predicted intercepts which are in much closer agreement with those deduced from the experimental results.

Equation 31 predicts that the values of  $f_n^-/n$  should also lie along a straight line on a plot of  $\log(f_n^-/n)$  versus  $(n-1)$ . Figure 7 shows that at 1 atm the point for methane lies well above the line given by eqn. 31, the points for  $n = 2$  through 8 fall below the line, and only the points for  $n = 9$  and 10 lie near the line. The agreement between theory and experiment is somewhat better at 10 atm. In this case Fig. 8 shows that the point for methane lies above the line, the points for  $n = 2$  and 3 lie below the line, but the points for  $n = 4$  through 8 lie along the line. The remaining two points, for  $n = 9$  and 10, lie slightly above the line. The pattern of the deviations between theory and experiment observed in Figs. 7 and 8 suggests that a part of the  $C_{2+}$  paraffinic product undergoes hydrogenolysis to form methane. Based on this interpretation, the correct value of  $f_1^-$  should be given by

$$f_1^- = (1-\alpha)^2 + \sum_{n=2}^{\infty} n [\alpha^{(n-1)} (1-\alpha)^2 - f_n^-/n] \quad (33)$$

Values of  $f_1^-$  determined in this fashion are listed in Table IV and are seen to be in good agreement with the values of  $f_1^-$  observed experimentally. The fact that the formation of excess methane is lower at higher pressure is consistent with the proposed interpretation. For the same  $H_2/CO$  ratio, elevation of the total pressure causes a reduction in  $\theta_v$ , due to the higher CO partial pressure, and, hence, a reduction in the availability of sites for paraffin adsorption. The decline in the extent of paraffin hydrogenolysis with increasing carbon number might be ascribed to the fact that with increasing molecular weight a higher number of contiguous vacant sites might be required for initial adsorption. Finally, it should be noted that in addition to explaining the discrepancies in the distribution of paraffins presented in Figs. 7 and 8, the occurrence of hydrogenolysis

would explain why in Figs. 2 and 3 the experimental points for  $n = 2$  and  $3$  fall below a straight line passed through the balance of the data.

The form of eqn. 27 indicates that plots of  $N_{C_n} = / N_{C_n}^{-0.5}$  versus  $P_{H_2}$  should result in straight lines with a slope of  $\beta$  which is independent of  $n$ . Figure 9 illustrates a test of this prediction for  $n = 2, 3,$  and  $4$ . The data plotted in this figure were taken at pressures between 1 and 10 atm and  $H_2/CO$  ratios between 1 and 3, and at temperatures of 498K to minimize the effects of olefin hydrogenation. For each value of  $n$  the data are seen to scatter around a straight line, in general agreement with eqn. 27 and consistent with the empirical rate expressions presented in Table I. It is apparent, though, that the slopes of the lines are dependent on the value of  $n$ . This dependence is seen even more clearly in Fig. 10 which shows a plot of  $\beta$  versus  $n$  for  $n = 2$  through 10. In the light of the discussion presented in connection with Figs. 7 and 8, it seems reasonable to propose that the high values of  $\beta$  for  $n = 2$  and  $3$  may be due, in part, to a partial hydrogenolysis of ethane and propane. The balance of the variation in  $\beta$  with  $n$  may be due to a dependence of the rate coefficients for chain termination on the value of  $n$ . A more detailed interpretation of these observations is not possible at present and must await further study.

The temperature dependence of  $N_{C_n} = / N_{C_n}$ , which was shown in Fig. 4, can be interpreted in terms of the rate and equilibrium constants appearing in the definition of  $\beta$ , eqn. 26. The difference in the apparent activation energies for the formation of olefins and paraffins,  $E_{op}$ , are related to the activation energies for the reactions of allyl species to form olefins and paraffins,  $E_o$  and  $E_p$ , and to the heat of  $H_2$  adsorption,  $\Delta H_{H_2}$ , by the following expression

$$E_{op} = E_o - E_p - \Delta H_{H_2} / 2 \quad (34)$$



Assuming that  $\Delta H_{H_2}$  is about -20 kcal/mole, a value typical for group VIII metals (35), leads to the conclusion that  $(E_p - E_o) \simeq 4$  kcal/mole.

A relationship for the dependence of  $\alpha$ , the probability of chain growth, on the partial pressures of  $H_2$  and CO can be determined starting from the definition for  $\alpha$ , eqn. 17. Substitution of eqns. 1, 4, 13, and 19 for  $\theta_v$ ,  $\theta_H$ ,  $\theta_{CH_2}$ , and  $\theta_O$  (assuming that  $N_{C_1} \ll \sum_{n=2}^{\infty} nN_{C_n}$ ) gives the following expression:

$$\alpha = [1 + \gamma(1-\alpha)^{-0.33} P_{CO}^{-0.67} (1 + \beta P_{H_2}^{-0.5})]^{-1} \quad (35)$$

where

$$\gamma = \left[ \frac{K_3}{k_p^2 k_4 K_1^2 K_2 K_5 K_6} \right]^{0.33} \quad (36)$$

Rearrangement of eqn. 36 provides a more explicit equation for  $\alpha$ , which can be solved by means of trial and error.

$$\alpha^{-1} (1-\alpha)^{1.33} = \gamma P_{CO}^{-0.67} (1 + \beta P_{H_2}^{-0.5}) \quad (37)$$

The utility of eqn. 37 as a representation for the dependence of  $\alpha$  on the partial pressures of  $H_2$  and CO, and on the temperature can now be examined. To do so requires that values of  $\beta$  and  $\gamma$  be determined first. An expression for  $\beta$  can be obtained from the data presented in Figs. 4 and 10. Choosing the value of  $\beta$  for  $n = 4$  as being representative leads to the following equation:

$$\beta = 1.8 \times 10^3 \exp(-5,700/RT) \quad (38)$$

An equation for  $\gamma$  can be obtained by forcing an agreement between eqn. 37 and the values of  $\alpha$  determined at 1 atm for  $H_2/CO = 2$  and temperatures of 498, 523, and 548K. The resulting expression is given by

$$\gamma = 1.2 \exp(-4,100/RT) \quad (39)$$

A comparison between the experimental and predicted values of  $\alpha$  is presented in Table V. It is observed that at 1 atm, eqn. 37 provides an accurate representation of the dependence of  $\alpha$  on temperature as well as  $H_2$  and CO partial pressures. When the total pressure is increased to 10 atm, eqn 37 predicts values of  $\alpha$  which are substantially higher than those observed experimentally. Nevertheless, the reduced dependence of  $\alpha$  on  $H_2$  and CO partial pressures observed at 10 atm is properly reflected.

The failure of eqn. 37 to provide an accurate estimation of  $\alpha$  at 10 atm is not well understood. A possible explanation might be that at higher pressures additional termination steps become important. Inspection of eqn. 17 shows that this would cause a decrease in  $\alpha$ . A reaction which might contribute to such an effect would be the insertion of CO into the metal-carbon bond of an alkyl group to form an acyl species which might subsequently react to produce either an aldehyde or an alcohol. Alternatively, one might consider the reaction of surface methylene or alkyl groups with olefins present in the reaction products (15,16). The results presented in Fig. 5 show that under the reaction conditions used in the present work, ethylene does not participate extensively in this type of reaction. However, this does not exclude the possibility that higher molecular weight olefins might be more reactive than ethylene. As a consequence further investigation will be needed to establish the effects of additional chain termination reactions and secondary reactions on the magnitude of  $\alpha$ .

#### CONCLUSIONS

In the present paper it has been shown that the reaction mechanism presented in Fig. 6 explains many aspects of CO hydrogenation over Ru. Rate expressions derived from this mechanism accurately describe the kinetics for the synthesis of methane and higher molecular weight hydrocarbons. It has been shown that  $C_{2+}$  olefins and paraffins are formed from a common pre-

cursor, and that, in the absence of further olefin hydrogenation, the olefin to paraffin ratio in the products depends only on the  $H_2$  partial pressure. It has also been demonstrated that the products in a homologous series follow a Schultz-Flory distribution. Minor deviations from such a distribution observed for olefins can be ascribed to a partial conversion of ethylene to ethane. The much more significant deviations found for paraffins appears to be due to a partial hydrogenolysis of  $C_{2+}$  alkanes, a process which seems to predominate at low CO partial pressures. Finally, it is concluded that the proposed mechanism can be used to deduce an expression for the effects of reaction conditions on the probability of chain growth,  $\alpha$ . This expression provides an excellent correlation of the experimental results obtained at 1 atm but overpredicts the values of  $\alpha$  observed at 10 atm. It is hypothesized that the discrepancy observed at higher pressures may indicate the presence of chain termination processes not included in the proposed mechanism.

#### ACKNOWLEDGMENT

The authors wish to express their appreciation to Prof. Earl Muetterties for the helpful discussions of the reaction mechanism proposed here. This work was supported by the Director, Office of Energy Research, Office of Basic Energy Sciences, Chemical Sciences Division of the U.S. Department of Energy, under Contract #W-7405-ENG-48.

#### REFERENCES

1. Vannice, M. A., Catal. Rev. Sci. Eng. 14, 153 (1976).
2. Ponec, V., Catal. Rev. Sci. Eng. 18, 151 (1978).
3. Ponec, V., and von Baneveld, W. A., I&EC Prod. Res. Develop. 18, 268 (1979).
4. Muetterties, E. L. and Stein, J., Chem. Rev. 80, 479 (1979).
5. Biloen, P., J. Roy. Neth. Chem. Soc. 99, 33 (1980).
6. Biloen, P. and Sachtler, W. M. H., Adv. Catal., in press.
7. Bell, A. T., Catal. Rev. Sci. Eng., in press.
8. Singh, K. J. and Grenga, H. E., J. Catal. 47, 328 (1977).

9. Rabo, J. A., Risch, A. P., and Poutsma, M. L., J. Catal. 53, 295 (1978).
10. Low, G., and Bell, A. T., J. Catal. 57, 397 (1979).
11. Biloen, P., Helle, J. N., and Sachtler, W. M. H., J. Catal. 58, 95 (1979).
12. Ekerdt, J. G. and Bell, A. T., J. Catal. 58, 170 (1979).
13. Kellner, C. S. and Bell, A. T., J. Catal., in press.
14. Brady III, G. and Pettit, R., J. Amer. Chem. Soc., in press.
15. Ekerdt, J. G. and Bell, A. T., J. Catal. 62, 19 (1980).
16. Baker, J. and Bell, A. T., unpublished results.
17. Kuznetsov, V. L., Bell, A. T., and Yermakov, Yu. I., J. Catal. 65 374 (1980).
18. Dalla Betta, R. A. and Shelef, M., J. Catal. 48, 111 (1977).
19. King, D. L., J. Catal. 61, 77 (1980).
20. Kellner, C. S. and Bell, A. T., submitted to J. Catal.
21. Cant, N. and Bell, A. T., unpublished results.
22. McCarty, J. G. and Wise, H., J. Catal. 60, 204 (1979).
23. Dalla Betta, R. A. Piken, A. G., and Shelef, M., J. Catal. 35, 53 (1974).
24. Vannice, M. A., J. Catal. 37, 449,462 (1975).
25. King, D. L., J. Catal. 51, 386 (1978).
26. Kellner, C. S., and Bell, A. T., submitted to J. Catal.
27. Friedel, R. A. and Anderson, R. B., J. Amer. Chem. Soc. 72, 1212,2307 (1950).
28. Henrici-Olive, G. and Olivé, S., Angew. Chem. Int. Ed. Engl. 15, 136 (1976).
29. Dautzenberg, I. M., Helle, J. N., von Santen, R. A. and Verbeck, H., J. Catal. 50, 8 (1977).
30. Anderson, R. B., J. Catal. 55, 114 (1978).
31. Madon, R. J., J. Catal. 57, 183 (1979).
32. Henrici-Olivé, G. and Olivé, S., J. Catal. 60, 481 (1979).
33. Anderson, R. B., J. Catal. 60, 484 (1979).
34. Madon, R. J., J. Catal. 60, 485 (1979).
35. Toyoshima, I., and Somorjai, G. A., Catal. Rev. Sci. Eng. 19, 105 (1979).

Table I. Dependencies of the Rates for the Synthesis of  $C_1$  through  $C_{10}$  Hydrocarbons on the Partial Pressures of  $H_2$  and  $CO^a$

$C_n$	Olefin			Paraffin		%Dev. <sup>b</sup>
	m	n	% Dev. <sup>b</sup>	m	n	
$C_1$	-	-	-	1.31	-0.96	7.7
$C_2$	0.82	-0.73	4.8	1.45	-0.85	7.7
$C_3$	0.80	-0.55	3.2	1.37	-0.49	4.9
$C_4$	0.74	-0.47	3.0	1.21	-0.46	3.3
$C_5$	0.53	-0.36	8.1	0.86	-0.24	2.3
$C_6$	0.47	-0.28	6.3	1.11	-0.32	13.5
$C_7$	0.35	-0.19	9.3	0.94	-0.24	5.9
$C_8$	0.31	-0.15	11.5	0.91	-0.27	7.9
$C_9$	0.20	-0.05	12.3	0.50	-0.18	19.4
$C_{10}$	0.17	-0.01	15.4	0.93	-0.35	11.4

<sup>a</sup>Reaction conditions:  $T = 498K$ ;  $P = 1-10$  atm;  $H_2/CO = 1-3$

<sup>b</sup>Average deviation between predicted and observed rates

Table II

Power Law Rate Expressions<sup>a</sup> for the Synthesis  
of C<sub>1</sub> through C<sub>4</sub> Hydrocarbons<sup>b</sup>

C <sub>n</sub>	A[atm <sup>(m-n)</sup> s <sup>-1</sup> ]	m	n	E <sub>a</sub> (kcal/mole)	%Dev. <sup>c</sup>
C <sub>1</sub>	1.3 x 10 <sup>9</sup>	1.35	-0.99	28	5.6
C <sub>2</sub> <sup>=</sup>	2.5 x 10 <sup>8</sup>	0.74	-0.68	28	5.7
C <sub>2</sub> <sup>-</sup>	1.6 x 10 <sup>6</sup>	1.34	-0.81	25	11.3
C <sub>3</sub> <sup>=</sup>	2.3 x 10 <sup>7</sup>	0.82	-0.58	25	4.2
C <sub>3</sub> <sup>-</sup>	1.4 x 10 <sup>3</sup>	1.39	-0.55	18	5.8
C <sub>4</sub> <sup>=</sup>	3.8 x 10 <sup>6</sup>	0.70	-0.44	24	9.6
C <sub>4</sub> <sup>-</sup>	8.7 x 10 <sup>3</sup>	1.14	-0.47	19	4.8

$$N_{C_n} = A \exp(-E_a/RT) P_{H_2}^m P_{CO}^n$$

b

Reaction conditions: T = 448-548K; P = 1-10 atm; H<sub>2</sub>/CO = 1-3.

c

Average deviation between predicted and observed rates

Table III

Comparison of the Rate Expressions for Methane Synthesis Obtained from Experimental Data with Those Obtained Theoretically

	Theory		This Study	Experiment		
	Eqn. 11	Eqn. 20		Dalla Betta et al. (23)	Vannice (24)	Ekerdt and Bell (12)
Catalyst	-	-	1% Ru/Al <sub>2</sub> O <sub>3</sub>	1.5% Ru/Al <sub>2</sub> O <sub>3</sub>	5% Ru/Al <sub>2</sub> O <sub>3</sub>	5% Ru/SiO <sub>2</sub>
A[atm <sup>(m-n)</sup> s <sup>-1</sup> ]	-	-	1.3 x 10 <sup>9</sup>	3.2 x 10 <sup>7</sup>	5.6 x 10 <sup>8</sup>	2.2 x 10 <sup>9</sup>
E <sub>a</sub> (kcal/mole)	-	-	28.2	24	24.2	24.1
m	1.5	1.5	1.35	1.8	1.6	1.5
n	-1.0	-1.33	-0.99	-1.1	-0.6	-0.6

Table IV

Comparison of the Observed Product Distributions with Schultz-Flory Distributions for Olefins and Paraffins

	P = 1 atm <sup>a</sup>		P = 10 atm <sup>a</sup>	
	Source	Value	Source	Value
$\alpha$	Fig. 7	0.62	Fig. 8	0.61
$\alpha$	Fig. 2	0.66	Fig. 3	0.63
$f_1^{\text{b}}$	Fig. 7	0.20	Fig. 8	0.23
$f_1^{\text{c}}$	$\frac{(1-\alpha)^2}{[1-(1-\alpha)^2]}$	0.18	$\frac{(1-\alpha)^2}{[1-(1-\alpha)^2]}$	0.17
$f_1^{\text{c}}$	See note c	0.21	See note c	0.21
$f_1^-$	Fig. 7	0.66	Fig. 8	0.44
$f_1^-$	$(1-\alpha)^2$	0.14	$(1-\alpha)^2$	0.18
$f_1^-$	See note d	0.64	See note d	0.41

<sup>a</sup>T = 498K; H<sub>2</sub>/CO = 3

<sup>b</sup>Intercept at (n-1) = 0

$$^c f_1^{\text{c}} = \frac{(1-\alpha)^2/[1-(1-\alpha)^2]}{\{1-2\{(1-\alpha)^2/[1-(1-\alpha)^2]-f_2^{\text{c}}/2\}\}}$$

$$^d f_1^- = (1-\alpha)^2 + \sum_{n=2}^{\infty} n[\alpha^{(n-1)}(1-\alpha)^2 - f_n^-/n]$$



Table V

Comparison of Predicted and Experimentally  
Observed Values of  $\alpha$

P(atm)	T(K)	H <sub>2</sub> /CO	$\alpha$	
			Predicted	Experimental
1	548	1	0.55	0.56
		2	0.52	0.51
		3	0.49	0.47
1	523	1	0.63	0.62
		2	0.60	0.61
		3	0.57	0.60
1	498	1	0.71	0.69
		2	0.68	0.68
		3	0.66	0.66
10	548	1	0.90	0.61
		2	0.89	0.60
		3	0.88	0.58
10	523	3	0.91	0.61
10	498	1	0.94	0.67
		2	0.94	0.63
		3	0.93	0.63

Figure Captions

- Fig. 1 Cross-plot of predicted versus observed rates of methane synthesis.
- Fig. 2 Distribution of  $C_1$  through  $C_{10}$  hydrocarbons observed at 1 atm:  
a) effects of  $H_2/CO$  ratio; b) effects of temperature
- Fig. 3 Distribution of  $C_1$  through  $C_{10}$  hydrocarbons observed at 10 atm:  
a) effects of  $H_2/CO$  ratio; b) effects of temperature.
- Fig. 4 Effects of temperature on the olefin to paraffin ratio of  $C_2$  through  $C_4$  products: a)  $P = 1$  atm; b)  $P = 10$  atm.
- Fig. 5 Effects of ethylene addition on the distribution of  $C_1$  through  $C_{10}$  hydrocarbons.
- Fig. 6 Proposed mechanism of hydrocarbon synthesis from CO and  $H_2$ .
- Fig. 7 Plots of  $f_n^-/n$  and  $f/n$  versus  $(n-1)$  for  $P = 1$  atm.
- Fig. 8 Plots of  $f_n^-/n$  and  $f_n^-/n$  versus  $(n-1)$  for  $P = 10$  atm.
- Fig. 9 Plots of  $N_{C_n}^-/N_{C_n}^-$  versus  $P_{H_2}^{-0.5}$ .
- Fig. 10 Plot of  $\beta$  versus  $n$

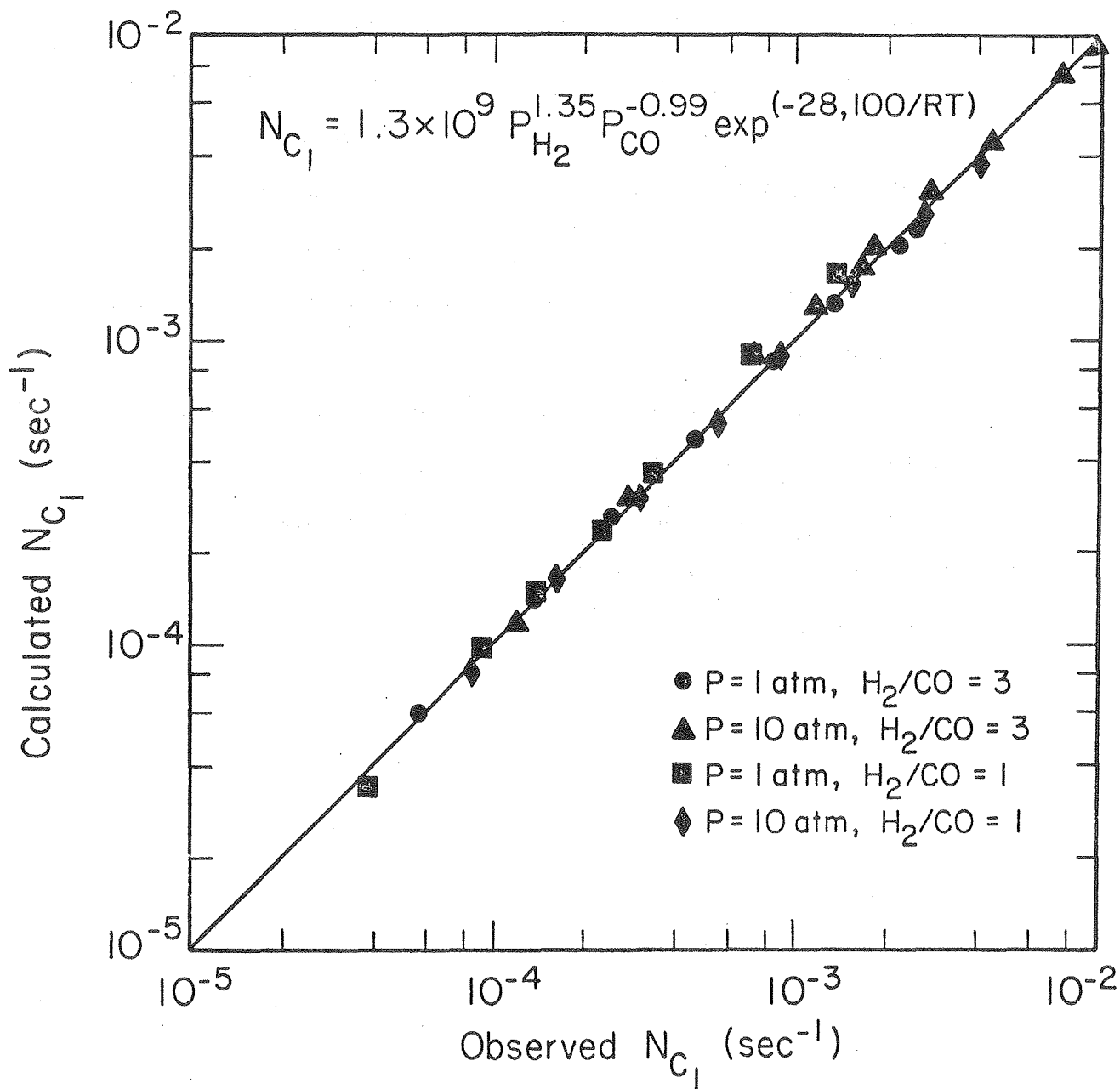


Fig. 1

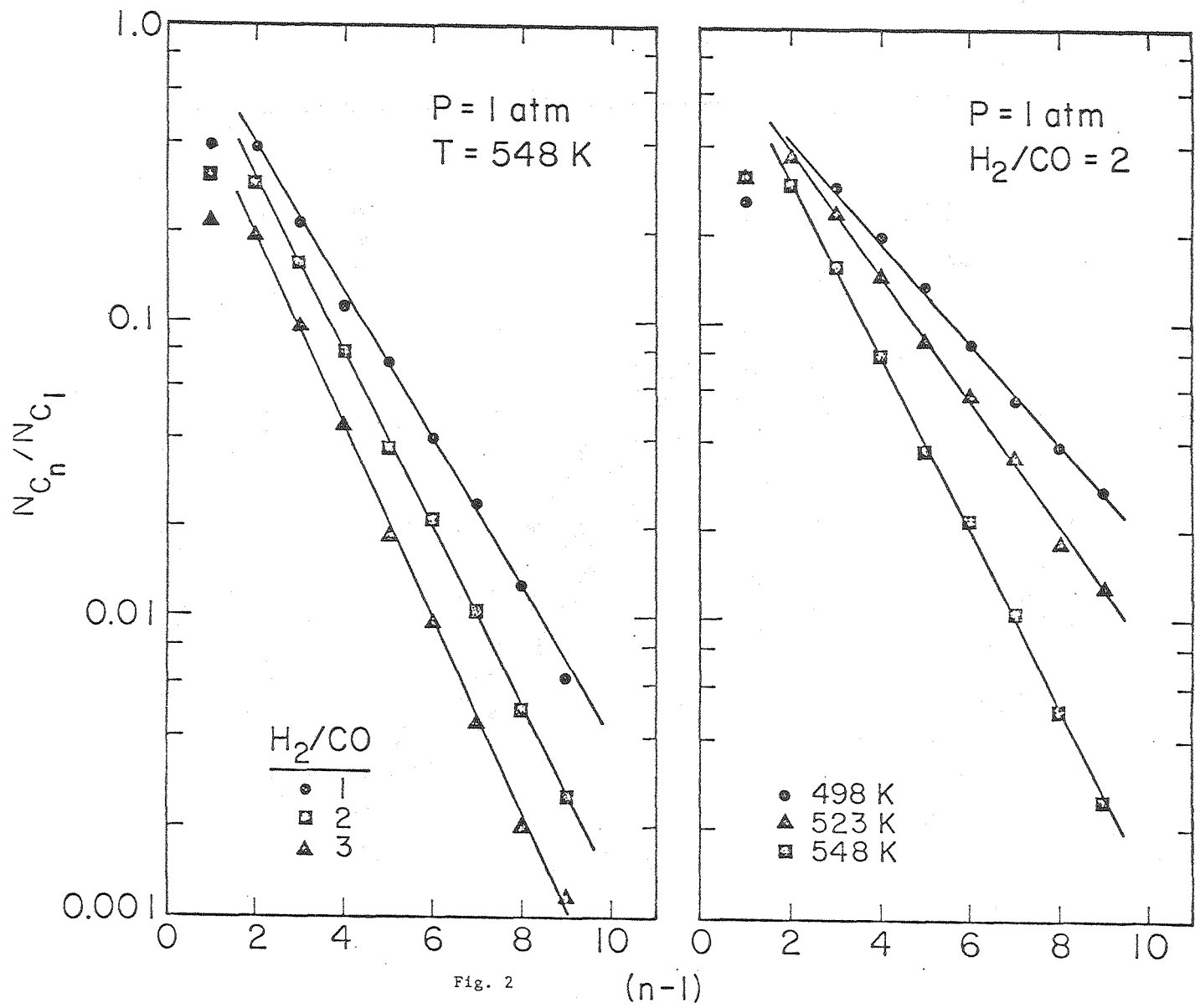


Fig. 2

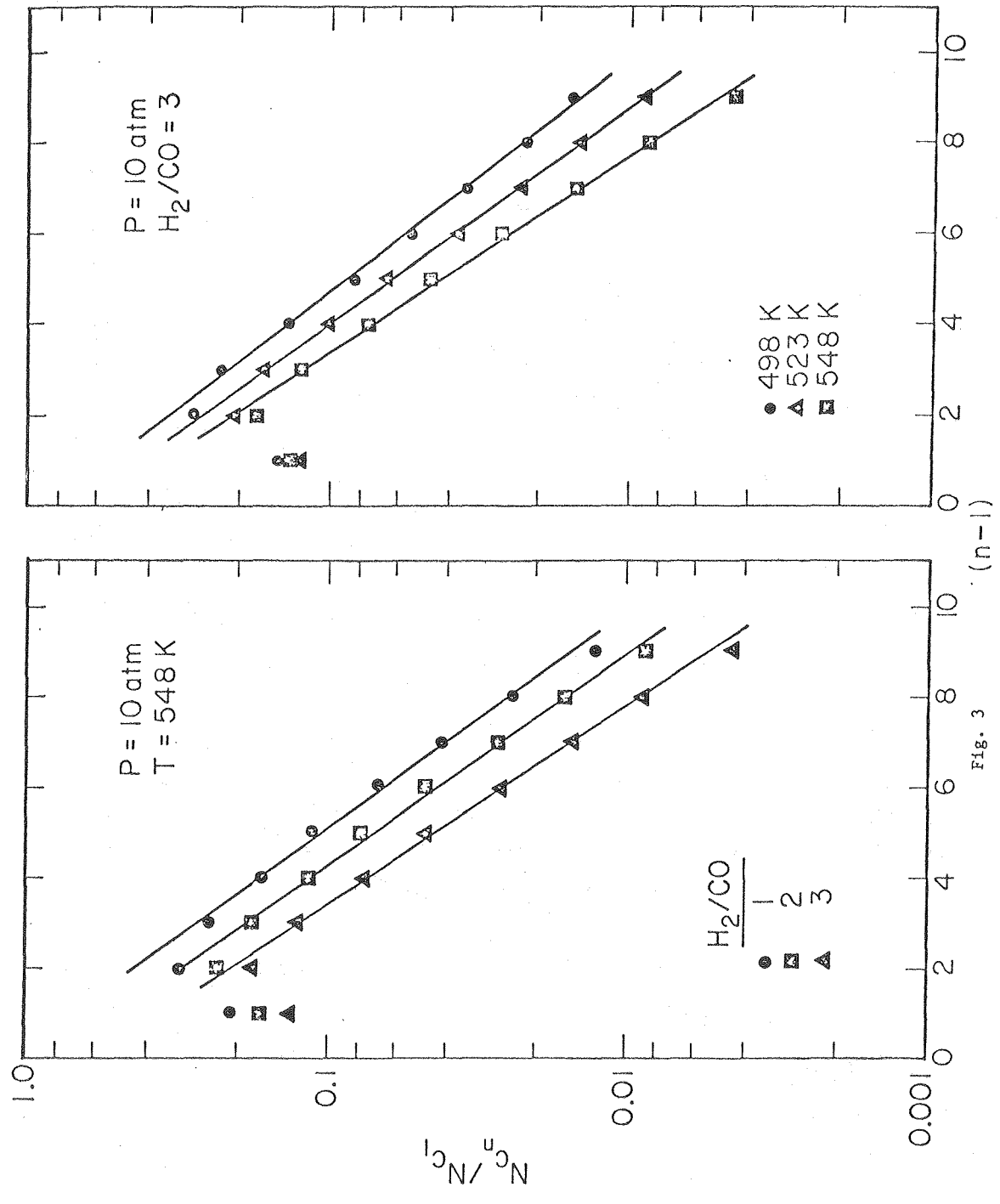


Fig. 3

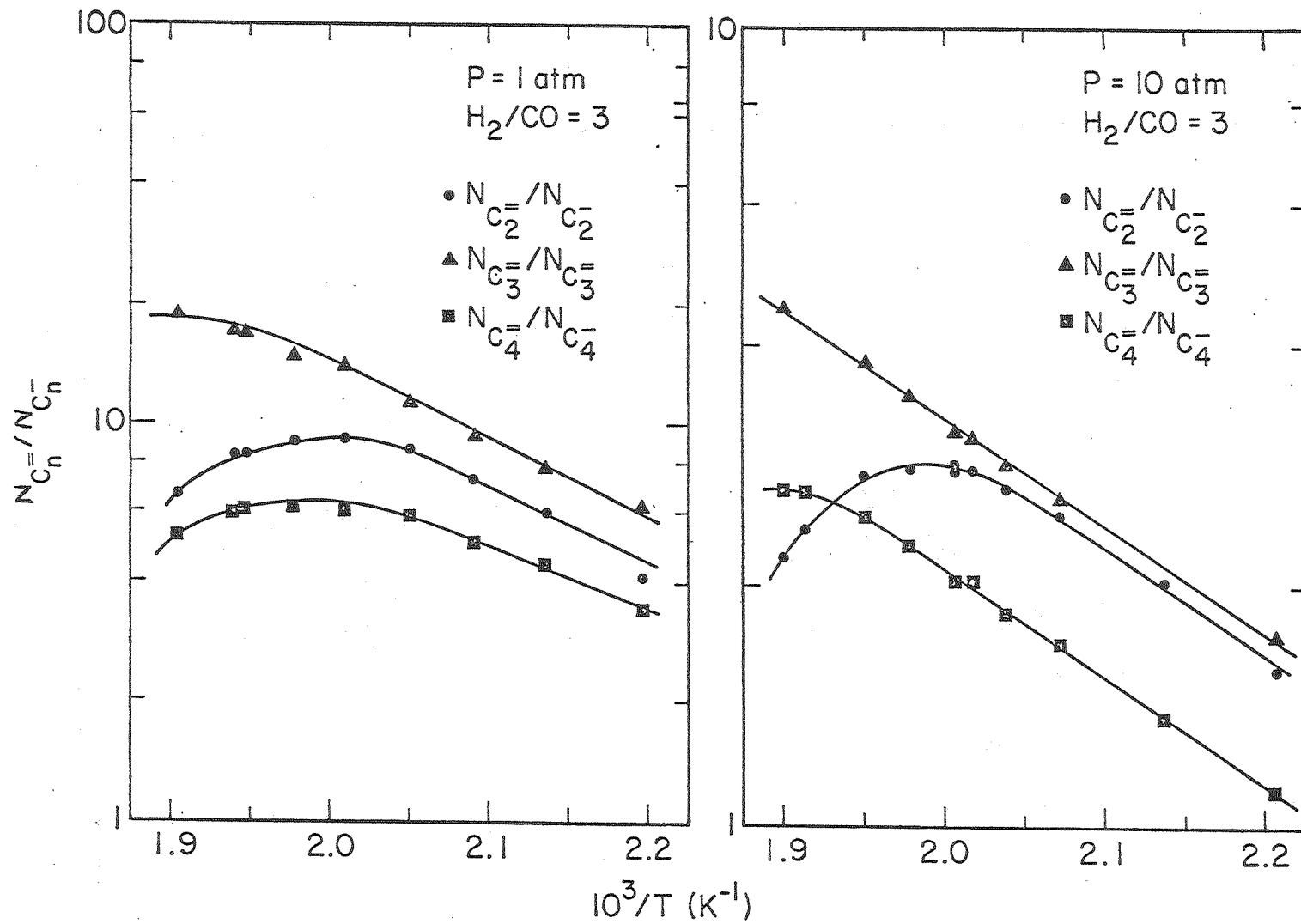


Fig. 4

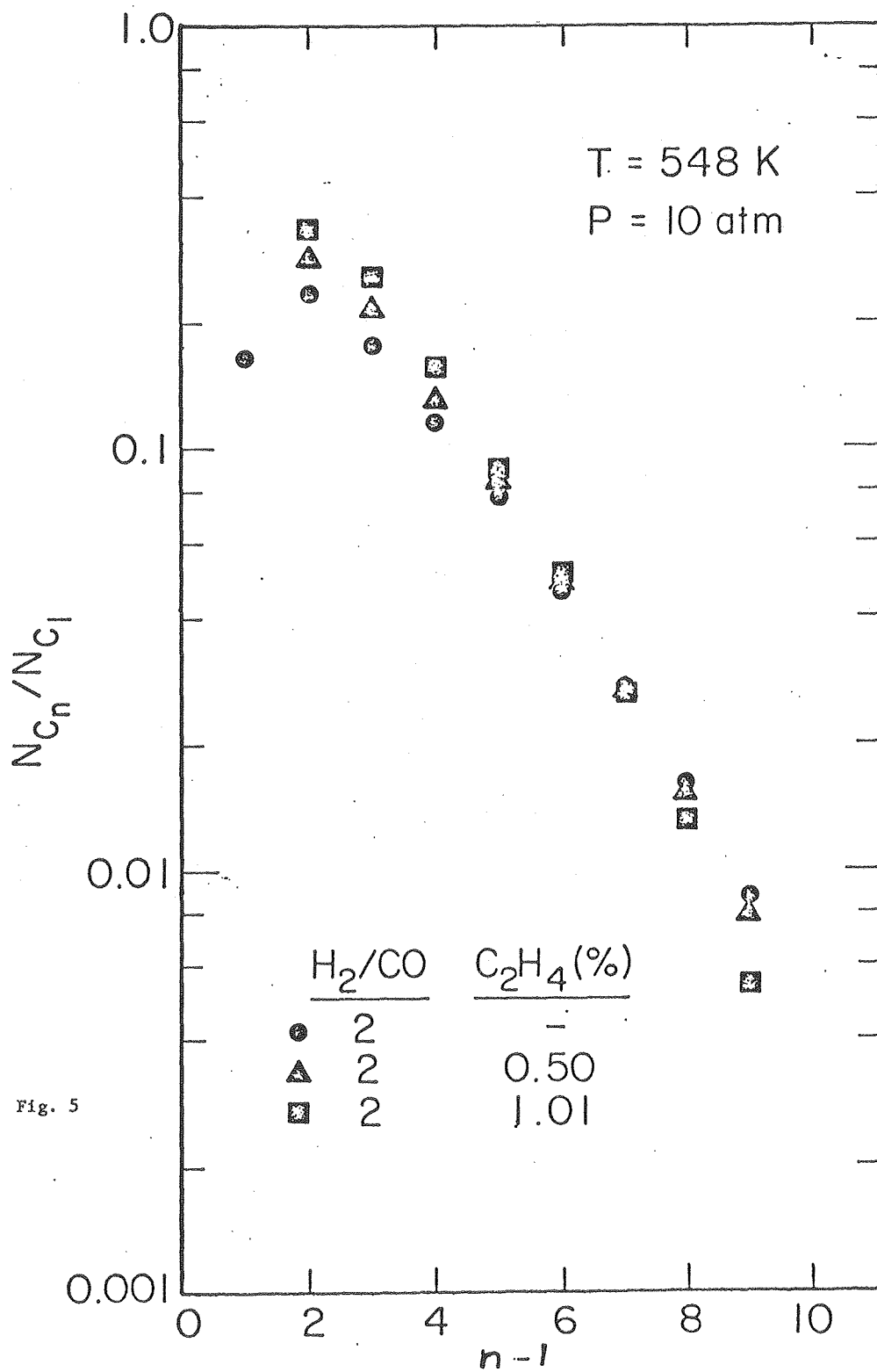
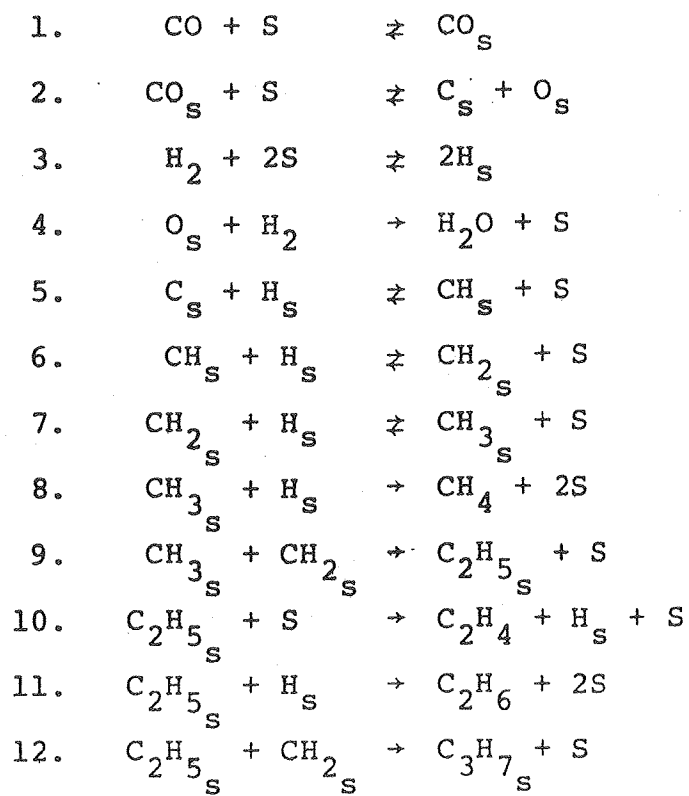


Fig. 5



etc.

Fig. 6



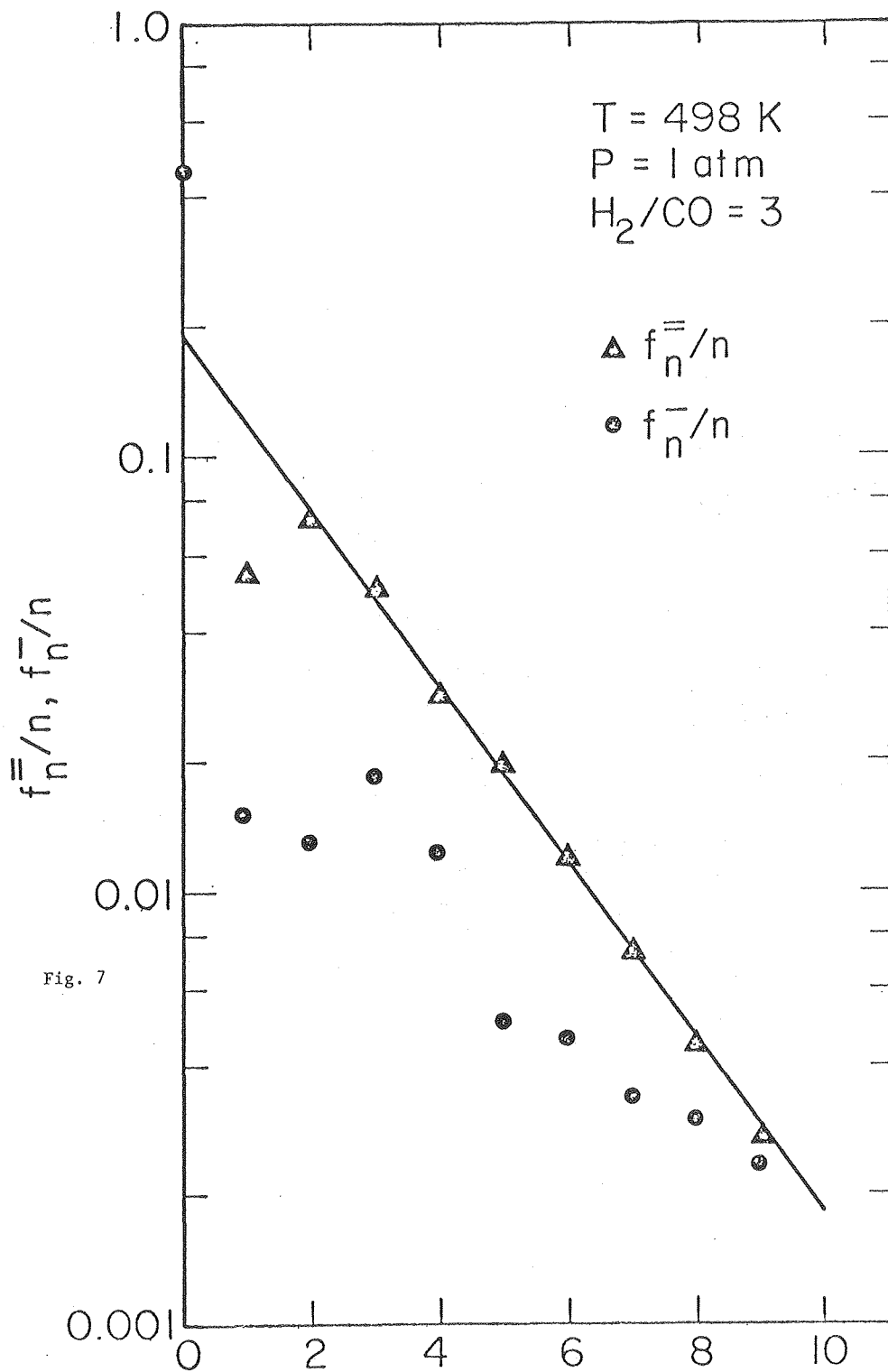


Fig. 7

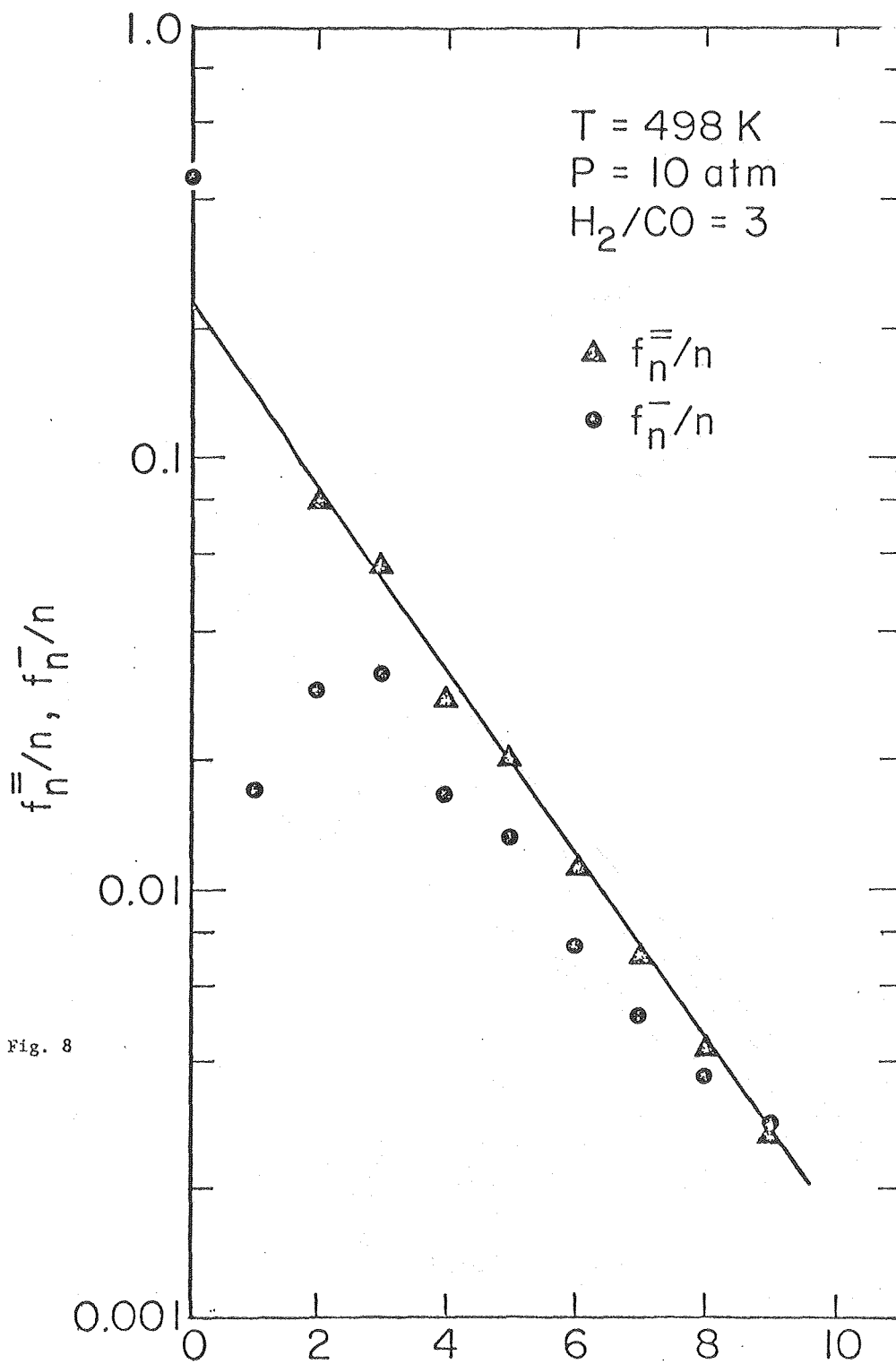


Fig. 8

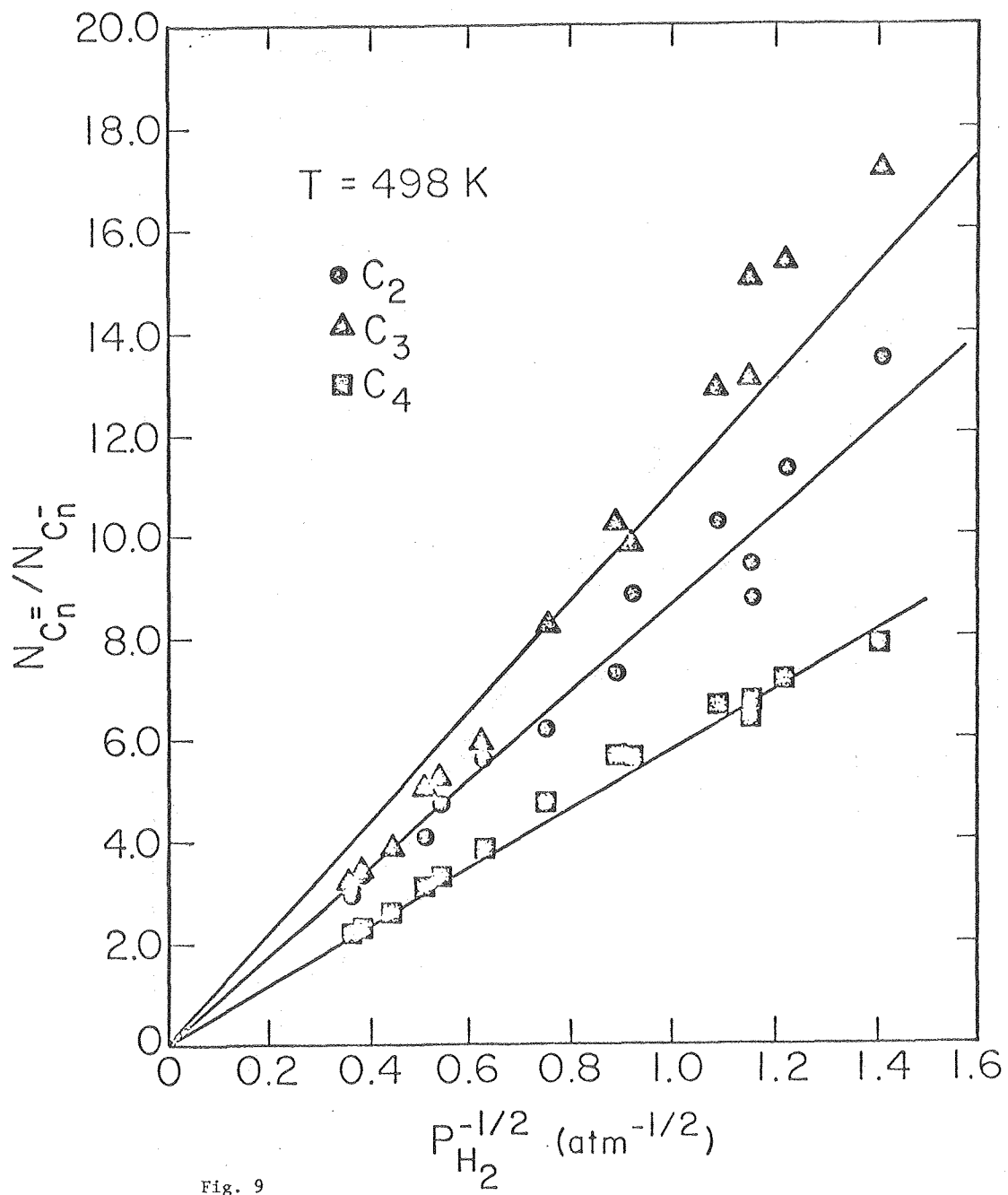


Fig. 9

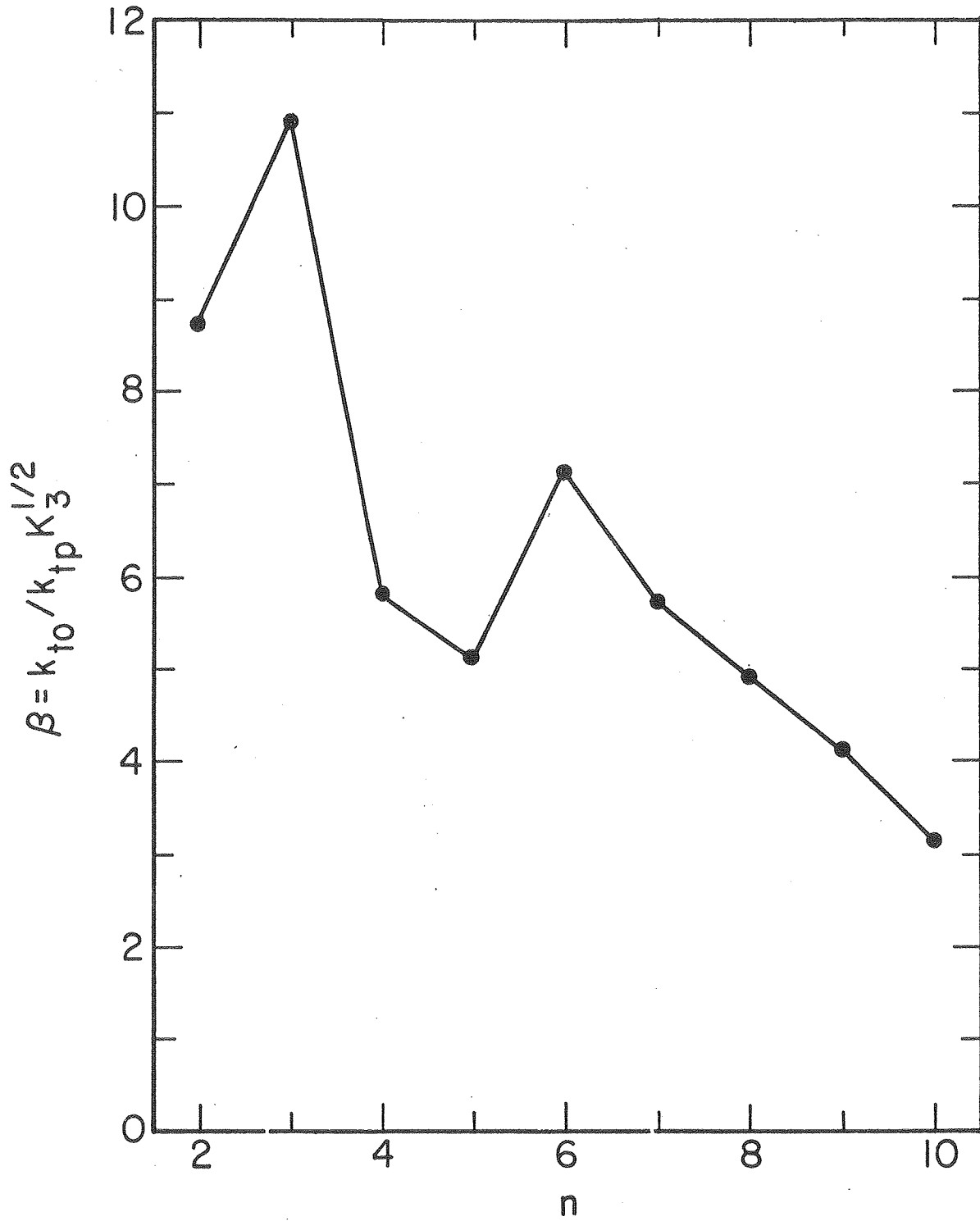


Fig. 10

